Inorganic Chemistry

pubs.acs.org/IC

Featured Article

Postsynthetic Modification of Half-Sandwich Ruthenium Complexes by Mechanochemical Synthesis

Wei-Guo Jia,* Xue-Ting Zhi, Xiao-Dong Li, Jun-Peng Zhou, Rui Zhong, Haibo Yu, and Richmond Lee*

Cite This: *Inorg. Chem.* 2021, 60, 4313−4321

Read Online

ACCESS | Metrics & More | Article Recommendations | Supporting Information

ABSTRACT: A mild and environmentally friendly method to synthesize half-sandwich ruthenium complexes through the Wittig reaction between an aldehyde-tagged half-sandwich ruthenium complex and phosphorus ylide mechanochemically is reported herein. The mechanochemical synthesis of valuable half-sandwich ruthenium complexes resulted in a fast reaction, good yield with simple workup, and the avoidance of harsh reaction conditions and organic solvents. The synthesized half-sandwich ruthenium complexes exhibited high catalytic activity for transfer hydrogenation of ketones using 2-propanol as the hydrogen source and solvent. Density functional theory was carried out to propose a mechanism for the transfer hydrogenation process. The modeling suggests the importance of the labile *p*-cymene ligand in modulating the reactivity of the catalyst.

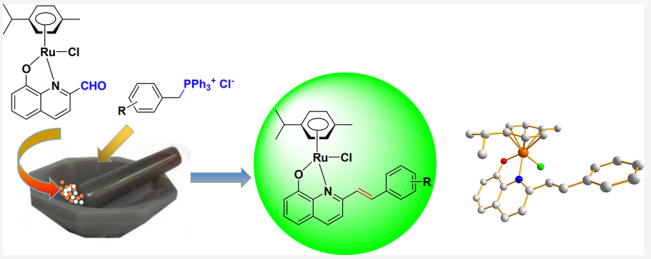

INTRODUCTION

The solvent-free synthesis of transition-metal complexes has recently gained considerable attention because it is more efficient and environmentally friendly.[1−5] Various coordination complexes including mononuclear and multinuclear complexes,[6−10] metal−organic frameworks,[11−13] covalent organic frameworks,[14] supramolecular compounds,[15,16] and coordination polymers[17−19] have been synthesized mechanochemically. However, using mechanochemistry to synthesize organometallic complexes is uncommon compared to the traditional solution or homogeneous method.[20−26] The synthesis of organometallic complexes in solution usually needs to be done under an inert atmosphere and in the absence of water and O_2 and requires the addition of pretreated solvents, coupled with a longer reaction time. The requirement of using dry and degassed solvents under inert reaction conditions increases the complexity of the reaction, adding to the cost of the synthesis, and generates a larger environmental footprint. The recent renaissance of mechanochemistry as a powerful synthetic tool can be used to overcome these problems to synthesize high-value products and organometallic-based catalysts.[27−30] Such solid-state mechanochemical reactions also eliminate the need to find suitable solvents to dissolve the reagents and other issues normally associated with solubility, enabling a wider variety of reagents to be used as molecular precursors. In short, mechanochemistry removes the need for solvents and also shortens the reaction time, leading to it being a more efficient and less polluting process. For example, Bantreil et al. recently reported the mechanochemical synthesis of half-sandwich ruthenium complexes with N-heterocyclic carbene (NHC) and $[Ru(p\text{-cymene})(\mu\text{-Cl})Cl]_2$, in situ obtaining the Ag-NHC complex with only a small amount of water (0.3 μL/mg of reactants).[31] Jurca and co-workers reported the mechanochemical synthesis of bis(imino)pyridine-MX_2 (M = Mn, Fe, Co, Ni, Cu, Zn; X = Cl, Br) complexes via a one-pot, one-step process from diacetylpyridine, panisidine, and a MX_2 precursor in the presence of $MgSO_4$ and *p*-toluenesulfonic acid.[32]

Following our interest in studying half-sandwich metal complexes' catalytic activities with diverse functional ligands,[33−37] we report herein an efficient and more sustainable method to synthesize a new, previously unreported half-sandwich ruthenium complex **2**, to the best of our knowledge. Complex **2** bears an aldehyde functional group that can enable postsynthetic modification, which could be carried out via a mechanochemical Wittig reaction. The resulting products of **4** (**4a** and **4b**) were obtained efficiently via mortar and pestle grinding, with the yields comparable to those of their solution-based methodologies. The ease of implementing such a solid-state postsynthetic modification of these organometallic complexes via simple grinding in air, without the need for expensive or sophisticated ball mills or a specialized mechanochemical apparatus, further highlights the attractiveness and feasibility of this methodology. The catalytic activities of the complexes were probed in transfer hydrogenation of ketones using 2-propanol as the hydrogen source and solvent. In particular, we discovered that complex **4b** demonstrated

Received: January 8, 2021
Published: March 24, 2021

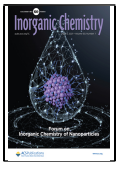

Scheme 1. Synthesis of Half-Sandwich Ruthenium Complexes with 2-Substituted 8-Hydroxyquinolinate Ligands through Mechanochemical and Solution Methods

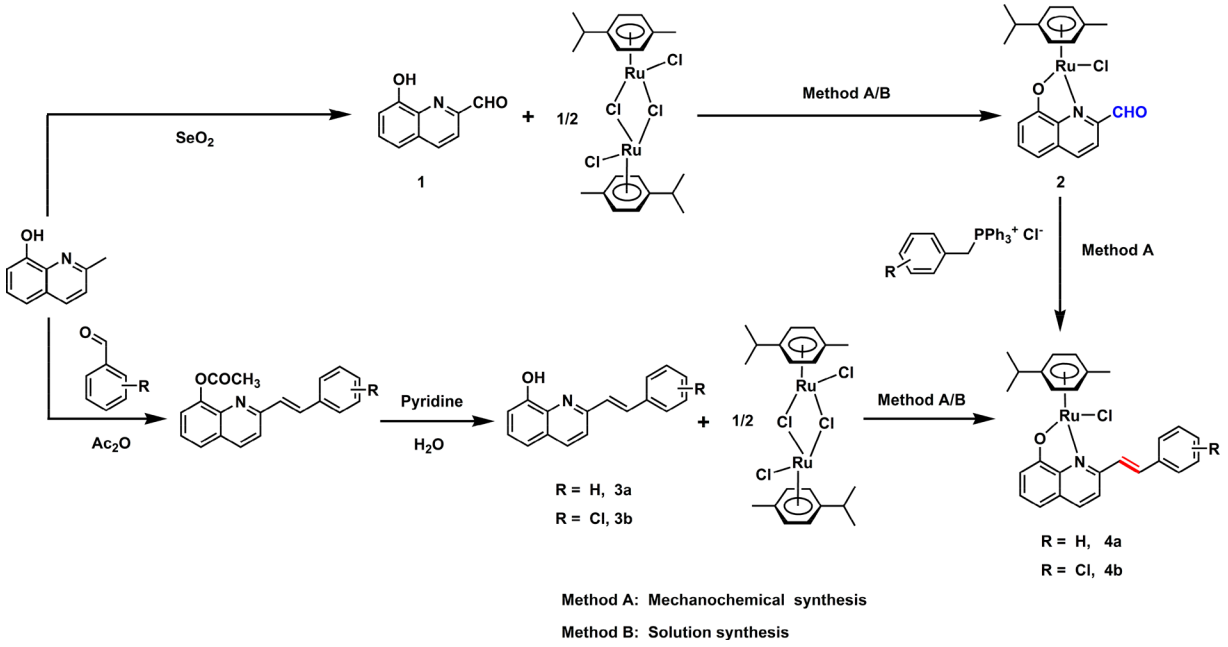

high catalytic activity for transfer hydrogenation of ketones with a broad range of substrates, forming a library of alcohol products that have significant synthetic value.

RESULTS AND DISCUSSION

Initially, the aldehyde-tagged half-sandwich ruthenium complex **2** was first obtained by the direct reaction between 8-hydroxyquinoline-2-carbaldehyde (**1**) and $[Ru(p\text{-cymene})(\mu\text{-}Cl)Cl]_2$ in solution using dry acetonitrile (MeCN) in an inert nitrogen atmosphere (Scheme 1). The ruthenium complex **2** was obtained in 62% yield after 2 h of continuous stirring at 70 °C. Alternatively, complex **2** was also obtained via the mechanochemical grinding of **1** and $[Ru(p\text{-cymene})(\mu\text{-}Cl)Cl]_2$ in the solid state. The mechanochemical protocol afforded **2** in higher yield (83%) and within a fraction of the time (20 min). The ruthenium complex **2** was fully characterized by Fourier transform infrared (FTIR), NMR spectroscopy, and mass spectrometry. As shown in Figure 1, complex **2** exhibits a strong stretching frequency at 1689 cm^{-1}, characteristic of the aldehyde ν(C═O). The proton signals at 10.70 ppm in the ^1H NMR spectrum can be easily assigned to the hydrogen atom of the −CHO group in complex **2** (Figure 2). Additionally, the electrospray ionization mass spectrometry (ESI-MS) spectrum of $[C_{20}H_{19}NO_2RuCl]^-$ exhibited peaks at m/z 442.0842 (calcd for $[M - H]^-$: m/z 441.9995), further confirming the formation of complex **2**. The aldehyde group in the ruthenium complex **2** provides a versatile and convenient " handle" for postsynthetic modification (Scheme 1).[38−41]

Next, we attempted to mechanochemically modify the ruthenium complex **2** postsynthetically. Complex **2**, in the presence of excess benzyltriphenylphosphonium chloride, afforded the desired complex **4a** in 62% yield by liquid-assisted grinding (LAG) in a mortar and pestle in air using two droplets of CH_2Cl_2 (approximate value of η = 0.0006 mL/mg).[42] The reaction proceeded readily and afforded complexes **4a** in open air without any special precautions. Ex situ FTIR measurements of the solid mixture allow for easy determination of the formation of the product. The C═C bond formation can be readily observed in the FTIR spectrum, as evidenced by the disappearance of the aldehyde ν(C═O) band and subsequent appearance of two new bands at 1633 and 968 cm^{-1}, which correspond to the ν(C═C) and trans ν(HC═CH) stretching frequencies, respectively (Figure 1). Complete conversion of the aldehyde was also confirmed by ^1H NMR data (Figure 2). The proton signal of the −CHO group observed in **2** at δ = 10.70 ppm was absent, and the other two new signals appeared as double peaks at δ = 7.69 and 7.51 ppm in the ^1H NMR spectrum of complex **4a**, indicating

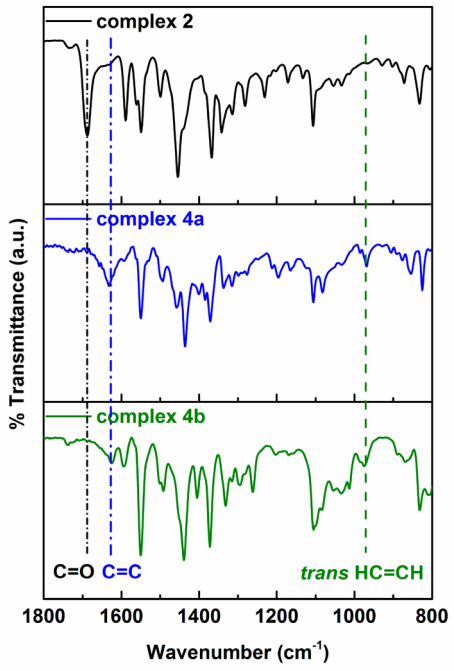

Figure 1. FTIR spectra of half-sandwich ruthenium complexes.

https://doi.org/10.1021/acs.inorgchem.1c00059
Inorg. Chem. 2021, 60, 4313−4321

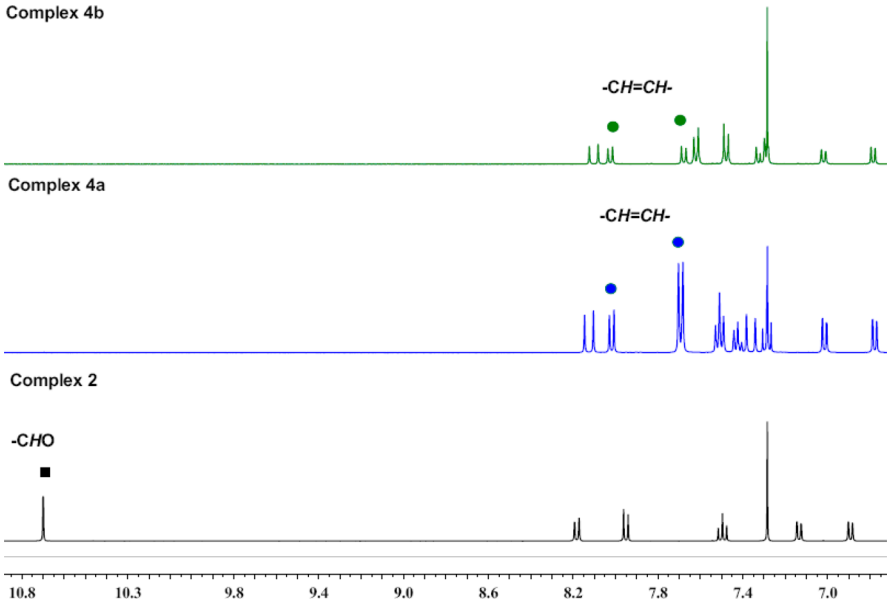

Figure 2. ^{1}H NMR spectra of half-sandwich ruthenium complexes.

C═C bond formation. Complex **4a** was also obtained by a mechanochemical ligand-exchange reaction between **3a** and $[Ru(p\text{-cymene})(\mu\text{-Cl})Cl]_2$ in 88% yield by LAG (Scheme 1). Similarly, postsynthetic modification of the ruthenium complex **2** via a Wittig reaction was also successively extended to [(4-chlorophenyl)methyl]triphenylphosphonium chloride under the same reaction conditions. Both FTIR and NMR analyses indicated that the reaction proceeded completely. Of note, the reaction involving **3b** completed within minutes under mechanochemical conditions, but took 3 h solvothermally to reach completion. Ex situ FTIR measurements revealed that the half-sandwich ruthenium complex **4** was immediately formed when a mixture of the ruthenium complex **2** and benzyltriphenylphosphonium chloride was ground under LAG at room temperature (Figure S10).

Subsequently, diffraction-quality crystals of **2**, **4a**, and **4b** were successfully grown and analyzed using single-crystal X-ray diffraction. The crystallographic data for compounds **2**, **4a**, and **4b** are summarized in Table S1, and selected key bond lengths and angles are shown in Table S2. The molecular structure of each complex was determined by X-ray crystallography and is shown in Figure 3, in which the chlorine atom, a nitrogen atom, and one oxygen atom each from the ligand and one of the *p*-cymene rings form a three-legged piano-stool geometry with Ru. The Ru−N distances [2.138(4) Å in **2**, 2.114(2) Å in **4a**, and 2.124(3) Å in **4b**] are in the range of typical distances of half-sandwich ruthenium complexes with a 8-hydroxyquinoline derivative.[43−47] The Ru−Cl distances [2.4087(14) Å in **2**, 2.4186(8) Å in **4a**, and 2.4112(9) Å in **4b**] are consistent with the Ru−Cl bond length values reported for those of half-sandwich ruthenium complexes.[48−51]

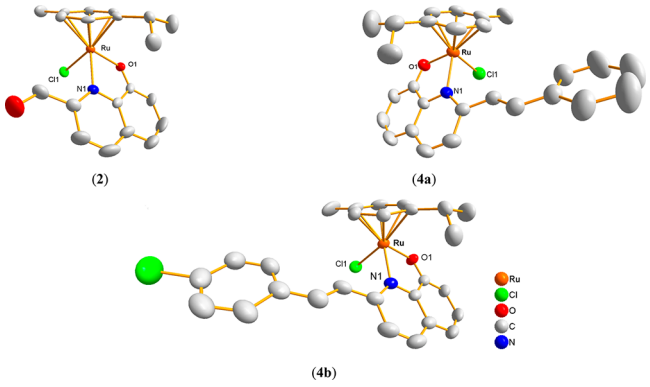

Figure 3. Molecular structures of complexes **2**, **4a**, and **4b**, with thermal ellipsoids drawn at the 50% level. All hydrogen atoms are omitted for clarity.

Transfer hydrogenation of acetophenone was chosen as the model reaction to test the catalytic activity of the obtained half-sandwich ruthenium complexes. The reaction was performed using 0.5 mol % catalyst loading in the presence of potassium *tert*-butoxide as the base under an inert nitrogen atmosphere. Optimization of the reaction parameters, as shown in Table 1, revealed that the ruthenium complex **4b** gave the best result, with a 39% yield within 3 h (Table 1, entries 1−3). A higher 91% yield was achieved when the reaction time was increased to 12 h at 0.25 mol % catalyst loading using **4b** (Table 1, entries 4 and 5). The type of base used was also crucial for the efficiency of this transformation, and sodium methoxide (MeONa) was found to be the ideal base for the transfer hydrogenation reaction of acetophenone (Table 1, entries 5−10). Lower yields were observed when the other inorganic bases such as KOAc, K_2CO_3, and K_3PO_4 were used. The reaction also proceeded more sluggishly when a lower reaction temperature was used (Table 1, entries 11 and 12). As a control reaction, the desired product was not detected in the absence of the half-sandwich ruthenium catalyst.

The transfer hydrogenation reaction was further extrapolated to other ketones under the optimized reaction conditions to evaluate the substrate scope of the catalytic system (Table 2). The reduction of a large variety of substrates, including aromatic and aryl alkyl/halide groups and aliphatic cyclic ketones, was efficiently performed. Ketones containing electron-withdrawing and -donating substituents on their aromatic backbone also afforded their corresponding products in excellent yields. Sterically bulky propiophenone and butyrophenone also afforded their corresponding alcohols in good yields (Table 2, entries 2 and 3), which means the steric

https://doi.org/10.1021/acs.inorgchem.1c00059
Inorg. Chem. 2021, 60, 4313−4321

Table 1. Optimization of Reaction Conditions for Transfer Hydrogenation of Acetophenone with Half-Sandwich Ruthenium Complexes[a]

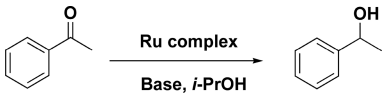

entry	catalyst	loading (mol %)	base	time (h)	temperature (°C)	yield (%)
1	**2**	0.5	tBuOK	3	80	24
2	**4a**	0.5	tBuOK	3	80	30
3	**4b**	0.5	tBuOK	3	80	39
4	**4b**	0.5	tBuOK	12	80	92
5	**4b**	0.25	tBuOK	12	80	91
6	**4b**	0.25	tBuONa	12	80	91
7	**4b**	0.25	MeONa	12	80	95
8	**4b**	0.25	KOAc	12	80	1
9	**4b**	0.25	K_2CO_3	12	80	4
10	**4b**	0.25	K_3PO_4	12	80	2
11	**4b**	0.25	MeONa	12	70	69
12	**4b**	0.25	MeONa	12	60	43

[a]Reaction conditions: acetophenone (0.1 mmol), catalyst, base (4 equiv), isopropyl alcohol (1 mL); *n*-dodecane as an internal standard. Determined by GC−MS.

hindrance of acetophenone did not have an influence on the catalytic activity of the reaction. While *p*- and *m*-methyl substituents did not hamper the reaction, a lower 72% yield was obtained for 2-methylacetophenone, even after prolonged reaction time (Table 2, entries 4−6). However, almost quantitative yields were observed for 2-acetoanisole (Table 2, entry 8). The transfer hydrogenation reaction also worked well for extended aromatic systems such as 2-acetylnaphthalene and 4-acetylbiphenyl and generated the corresponding products in excellent yields (Table 2, entries 11 and 12). Halide or trifluoromethyl substituents on the ortho, meta, or para position of the aromatic ring were also allowed (Table 2, entries 13−20). The catalyst also tolerated reagents with hydroxy groups, as shown in 2-hydroxy-2-methylpropiophenone, albeit with slightly lower obtained product yield (84% yield; Table 2, entry 21). Notably, sterically hindered fluoren-9-one was also efficiently reduced to fluoren-9-ol (Table 2, entry 22). Also, the heterocycle substrate was tolerated well (Table 2, entry 23). The aliphatic compound 4-*tert*-butylcyclohexanone was also successfully reduced to 4-*tert*-butylcyclohexanol in excellent yield (Table 2, entry 24).

Density functional theory (DFT; see the Supporting Information for computational details) was carried out to shed light and propose a plausible mechanism for the transfer hydrogenation process, with **4b** catalyst, MeO^- base, and acetophenone chosen for the computational modeling (Figure 4). The facile exchange of Cl^- in **4b** with MeO^- leads to the methoxyl complex **cpxA**, and all free energies will be referenced to **cpxA** henceforth. The hydrogen-bonded methoxyl complex with 2-propanol (**cpxB**) is slightly exergonic, and further exchange of the methoxide and 2-propanol leads to **cpxC**. Both **cpxB** and **cpxC** are slightly less stable compared to **cpxA**, and *β*-hydride elimination of the 2-propanolate in **cpxC** requires one to overcome a high activation barrier of $\Delta G^{\ddagger}$ = 31.1 kcal/mol ($\Delta G_{sol}^{\ddagger}$ = 28.9 kcal/mol) relative to **cpxA** (see Figure 4, Pathway A). An energetically stable Ru−H species **cpxD** is formed. The subsequent reduction of acetophenone from **cpxD** via **TSD** is also high in the activation barrier at $\Delta G^{\ddagger}$ = 34.6 kcal/mol ($\Delta G_{sol}^{\ddagger}$ = 37.5 kcal/mol) relative to **cpxD**. An alternative pathway (see Figure 4, Pathway B) whereby the cymene ligand is substituted with alcohols to give a 16-electron ruthenium(II) trigonal-bipyramidal complex **cpxE** is also considered.[37] This **cpxE** species is endergonic but has a vacant site available for accepting a hydride, which then sets the stage for *β*-hydride elimination through **TSE**: $\Delta G^{\ddagger}$ = 20.3 kcal/mol ($\Delta G_{sol}^{\ddagger}$ = 20.9 kcal/mol). A **TSE** activation barrier being much lower than **TSC** is proposed to be operative. The formed Ru−H species **cpxF** is, however, unstable and could undergo ligand substitution, with the cymene coming back to form stable **cpxD** as a resting state, ΔG = −3.7 kcal/mol (ΔG_{sol} = −5.8 kcal/mol). For the next step of transfer hydrogenation to occur, ligand substitution between the labile cymene of **cpxD** and acetophenone forms the precomplex **cpxG**, which is more stable compared to **cpxF**. The reduction of acetophenone from **cpxG** through **TSG** is energetically lower at $\Delta G^{\ddagger}$ = 18.8 kcal/mol ($\Delta G_{sol}^{\ddagger}$ = 24.5 kcal/mol) relative to **cpxD**. The reduced methylbenzyl alcohol on **cpxH** is protonated, forming **cpxI**, and expulsion of methylbenzyl alcohol and 2-proponal and coordination with cymene regenerate **cpxA**, giving an overall exergonic process.

On the basis of the calculations, the lability of the cymene ligand is important in influencing the reactivity of the ruthenium catalyst, allowing transfer hydrogenation steps to occur when it is not coordinated to the ruthenium metal center. However, if the ligand is on the metal center, the energetics for hydrogen transfer will be unfavorable (see Figure 4, Pathway A). The electron-deficient bipyramidal 16-electron ruthenium(II) complexes are unstable but reactive, and sterics play a role in this; the *trans*-alkene group on the **3b** ligand blocks another ligand from coordinating to the metal, preventing a full 18-electron ruthenium species. Thus, the energetically stable 18-electron piano-stool cymene−ruthenium complexes **cpxD** and **cpxA** are proposed to be present as stable intermediates in order to drive the reaction forward.

CONCLUSION

The mechanosynthesis of organometallic half-sandwich ruthenium complexes **4**, including from postsynthetic modification of the aldehyde-tagged half-sandwich ruthenium complex **2**, has been successfully demonstrated. The mechanochemical methodology for the synthesis of complex **4** was very efficient, with up to 20% higher isolated yield than its solution-based counterpart. The molecular structures of all half-sandwich ruthenium complexes were confirmed by spectroscopic and X-ray diffraction studies. Complex **4b** was discovered to exhibit high catalytic activity toward transfer hydrogenation of ketones to alcohols, using 2-propanol as the hydrogen source and solvent. DFT was used to computationally model and propose a mechanism for this transformation. Theoretical insights suggest the importance of the lability of the cymene ligand toward modulation of the reactivity of the catalyst. A large library of synthetically valuable alcohol products were generated using the optimal catalyst. The success of adopting mechanochemistry in our synthetic protocols has given us the confidence to explore further other reactions involving analogous organometallic compounds, and we hope that this work will further encourage more organometallic chemists to consider using mechanochemistry as part of their toolbox of synthetic methodologies.

https://doi.org/10.1021/acs.inorgchem.1c00059
Inorg. Chem. 2021, 60, 4313−4321

Table 2. Screening of Substrates for Transfer Hydrogenation of Ketone Compounds Catalyzed by Complex 4b[a]

Entry	Substrate	Product	Yield (%)	Entry	Substrate	Product	Yield (%)
1	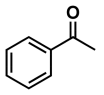	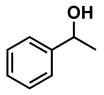	95	13	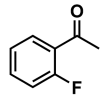	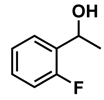	99
2	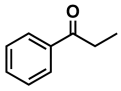	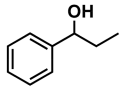	97	14	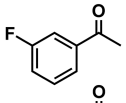	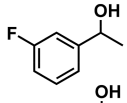	99
3	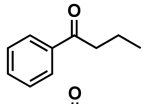	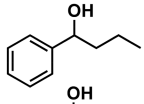	99	15	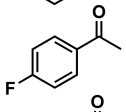	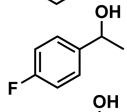	99
4[c]	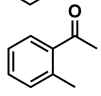	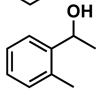	72	16	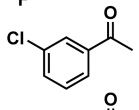	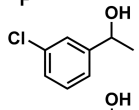	99
5	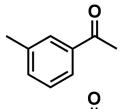	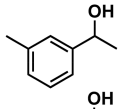	91	17	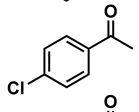	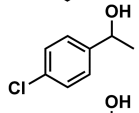	99
6	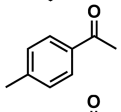	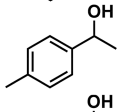	99	18	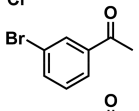	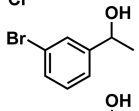	99
7	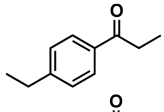	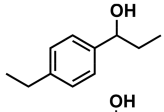	96	19	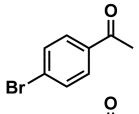	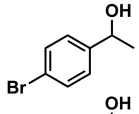	99
8	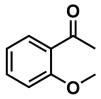	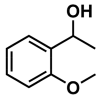	99	20	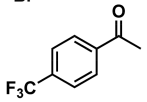	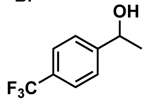	99
9	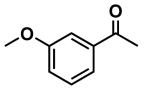	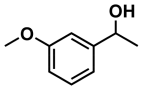	99	21	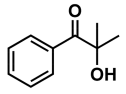	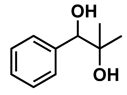	84
10	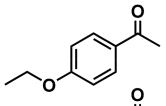	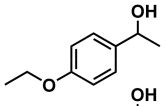	83	22	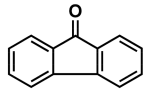	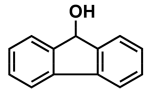	99
11			99	23			86
12			93	24			99

[a]Reaction conditions: ketones (0.1 mmol), catalyst (0.25 mol %), MeONa (4 equiv), isopropyl alcohol (1 mL), 80 °C, 12 h; *n*-dodecane as an internal standard. [b]The yields were determined by GC−MS. [c]24 h.

EXPERIMENTAL SECTION

Materials and measurements. All operations were carried out under an inert nitrogen atmosphere using standard Schlenk techniques. All solvents were purified and degassed by standard procedures. The compounds 8-hydroxyquinoline-2-carbaldehyde (**1**),[52] 2-styryl-8-hydroxyquinoline (**3a**),[53,54] 2-(4-chlorostyryl)-quinolin-8-ol (**3b**),[55,56] [(4-chlorophenyl)methyl]-triphenylphosphonium chloride,[57] and benzyltriphenylphosphonium chloride[58] were synthesized according to the literature. ^{1}H and ^{13}C NMR were recorded on a Bruker AV 400/500 spectrometer at room temperature. Chemical shifts (δ) are given as parts per million (ppm) and refer to the shift of the hydrogen or carbon atoms in the solvents used ($CDCl_3$). The following abbreviations were used for assignment of the signals and their multiplicities: s, singlet; d, doublet; t, triplet; q, quartet; m, multiplet. The given coupling constants *J* are listed as the average of the experimental findings. The FTIR (KBr pellet) spectrum was recorded (400−4000 cm^{-1} region) on a Bruker TENSOR 27 FTIR spectrometer. Elemental analyses were performed on a PerkinElmer 2400 CHN analyzer. ESI-MS spectra were recorded on Bruker micrOTOF-Q II 10280 and Bruker micrOTOF II 10257 mass spectrometers.

Synthesis of the Half-Sandwich Ruthenium Complex ***2***. **Method A** (mechanochemical synthesis method): $[Ru(p\text{-cymene})(\mu\text{-Cl})Cl]_2$ (61.2 mg, 0.10 mmol), **1** (0.2 mmol), and K_2CO_3 (27.6 mg, 0.2 mmol) were manually ground in a mortar with a pestle for 20 min in the presence of 5 droplets of CH_2Cl_2. The resulting products was poured into a CH_2Cl_2 solution, and any precipitate that formed was removed by filtration. The solvent in the resulting filtrate was removed in vacuo. The mixture was passed through a short pad of silica gel with hexane and isopropyl alcohol to give the ruthenium complex **2** (73.6 mg, 83%). **Method B** (solution method): A solution of $[Ru(p\text{-cymene})(\mu\text{-Cl})Cl]_2$ (61.2 mg, 0.10 mmol), **1** (0.22 mmol), and K_2CO_3 (35.4 mg, 0.22 mmol) in MeCN (5 mL) was purged with nitrogen and then stirred at 70 °C for 2 h. After the solution was cooled to room temperature, the solvent was removed under vacuum (rotary evaporator). The mixture was passed through a short pad of silica gel with ethyl acetate and petroleum ether (2:1) to give the characteristic dark-red half-sandwich ruthenium complex **2** (55.0 mg, 62%). ^{1}H NMR (500 MHz, $CDCl_3$): δ 10.67 (s, 1H), 8.14 (d, 1H),

https://doi.org/10.1021/acs.inorgchem.1c00059
Inorg. Chem. 2021, 60, 4313−4321

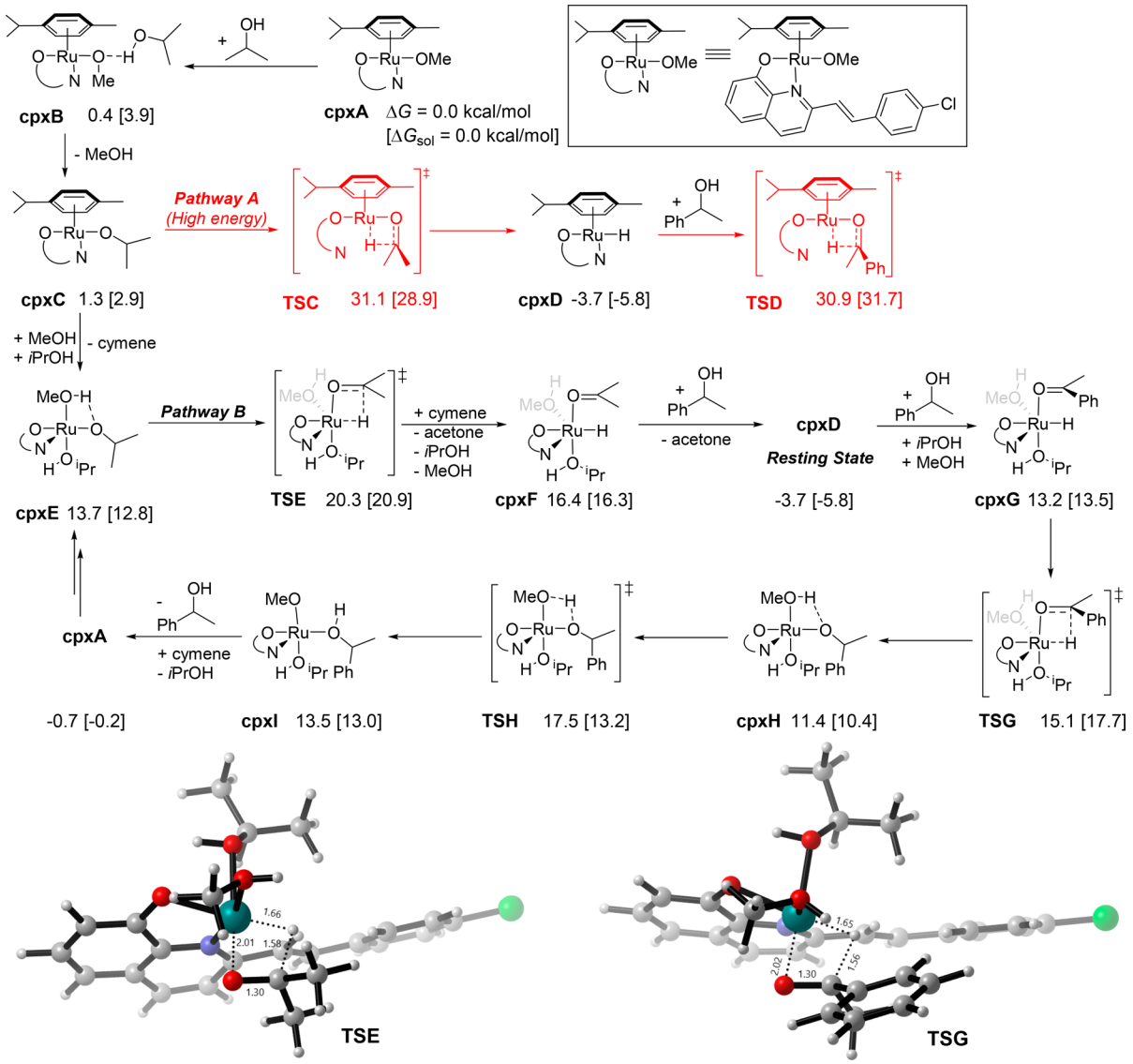

Figure 4. Top: Computational modeling of the reaction mechanism for transfer hydrogenation catalyzed by **4b**. Values are gas-phase free energies at the M11-L/def2TZVP+QZVP level of theory on optimized minimum or transition-state structures at M11-L/6-31G(d,p)+SDD [solution free energy calculation with implicit 2-propanol solvation in square brackets]. Bottom: Transition-state structures **TSE** and **TSG** and bond distances for hydrogen transfer.

7.91 (d, 1H), 7.44 (t, 1H), 7.09 (d, 2H), 6.86 (d, 2H), 5.69 (d, 1H), 5.57 (d, 1H), 5.26 (q, 2H), 2.51 (m, 1H), 2.31 (s, 3H), 1.00 (d, J = 9 Hz, 3H), 0.92 (d, J = 15 Hz, 3H). ^{13}C NMR (125 MHz, $CDCl_3$): δ 192.7, 169.6, 150.0, 145.1, 138.4, 133.4, 131.6, 120.2, 116.7, 111.0, 103.0, 101.0, 85.7, 81.7, 81.5, 80.4, 31.3, 22.4, 19.1. IR (KBr cm^{-1}): 3434 (m), 3057 (w), 2965 (w), 2924 (vw), 2873 (w), 1733 (vw), 1687 (s), 1589 (m), 1549 (s), 1499 (m), 1453 (s), 1368 (s), 1342 (s), 1313 (m), 1280 (m), 1229 (m), 1169 (m), 1108 (s), 872 (m), 832 (m), 739 (m), 598 (m), 509 (m). Anal. Calcd for $C_{20}H_{20}NO_2RuCl$: C, 54.24; H, 4.55; N, 3.16. Found: C, 54.28; H, 4.47; N, 3.10. ESI-MS. Calcd for $[C_{20}H_{19}NO_2RuCl]^-$ ($[M - H]^-$): m/z 441.9995. Found: m/z 442.0842.

Synthesis of the Half-Sandwich Ruthenium Complex ***4a.*** **Method A** (mechanochemical synthesis method): Benzyltriphenylphosphonium chloride (77.6 mg, 0.2 mmol) and potassium *tert*-butoxide (33.7 mg, 0.3 mmol) were manually ground in a mortar with a pestle for 1 min, until a yellow solid was obtained. Then, **2** (42.7 mg, 0.1 mmol) was added to the solid mixture and subsequently ground for 1 h in the presence of 2 droplets of CH_2Cl_2. The resulting products were poured into a CH_2Cl_2 solution, the unsolved precipitate was removed by filtration, and the solvent in the filtrate was removed in vacuo. The mixture was passed through a short pad of silica gel with hexane and isopropyl alcohol to give the ruthenium complex **4a** (30.1 mg, 62%). **Method A** (mechanochemical synthesis method): $[Ru(p\text{-cymene})(\mu\text{-Cl})Cl]_2$ (61.2 mg, 0.10 mmol), **3a** (0.2 mmol), and K_2CO_3 (27.6 mg, 0.2 mmol) were manually ground in a mortar with a pestle for 20 min in the presence of 5 droplets of CH_2Cl_2. The resulting products were poured into a CH_2Cl_2 solution, the unsolved precipitate was removed by filtration, and the solvent was removed in vacuo. The mixture was passed through a short pad of silica gel with hexane and isopropyl alcohol to give the ruthenium complex **2** (91.6 mg, 88%). **Method B** (solution method): A solution of $[Ru(p\text{-cymene})(\mu\text{-Cl})Cl]_2$ (61.2 mg, 0.10 mmol), **3a** (0.22 mmol), and K_2CO_3 (35.4 mg, 0.22 mmol) in methanol (5 mL) was purged with nitrogen and then stirred at 70 °C for 2 h. After it was cooled to room temperature, the solvent was removed under vacuum (rotary evaporator). The mixture was passed through a short pad of silica gel with ethyl acetate and petroleum ether (2:1) to give the dark-red half-sandwich ruthenium complex **4a** (70.9 mg, 69%). ^{1}H NMR (400 MHz, $CDCl_3$): δ 8.13 (d, J = 20 Hz, 1 H), 8.02 (d, J = 8 Hz, 1 H), 7.69 (d, J = 8 Hz, 3 H), 7.51 (t, J = 16 Hz, 2 H), 7.42 (t, J = 12 Hz, 1 H), 7.36 (d, J = 16 Hz, 1 H), 7.29 (t, J = 16 Hz, 1 H), 7.02 (d, J = 12

https://doi.org/10.1021/acs.inorgchem.1c00059
Inorg. Chem. 2021, 60, 4313−4321

Hz, 1 H), 6.78 (d, J = 8 Hz, 1 H), 5.62 (d, J = 4 Hz, 1 H), 5.51 (d, J = 4 Hz, 1 H), 5.39 (d, J = 8 Hz, 1 H), 5.14 (d, J = 4 Hz, 1 H), 2.57 (m, 1 H), 2.33 (s, 3 H), 1.03 (d, J = 8 Hz, 3 H), 0.94 (d, J = 4 Hz, 3 H). ^{13}C NMR (100 MHz, $CDCl_3$): δ 168.6, 155.8, 144.3, 137.5, 135.9, 134.0, 131.0, 129.7, 129.2, 128.6, 127.4, 119.9, 115.7, 110.5, 101.4, 100.2, 85.6, 81.0, 80.9, 80.3, 30.8, 22.2, 22.0, 18.9. IR (KBr cm^{-1}): 3432 (m), 3063 (vw), 2958 (m), 2923 (s), 2854 (m), 1632 (w), 1549 (m), 1493 (w), 1457 (w), 1436 (m), 1370 (m), 1195 (vw), 1105 (w), 1082 (w), 969 (vw), 852 (w), 823 (w), 741 (w), 691 (w), 512 (w). Anal. Calcd for $C_{27}H_{26}NORuCl$: C, 62.72; H, 5.07; N, 2.71. Found: C, 62.77; H, 5.09; N, 2.78. ESI-MS. Calcd for $[C_{27}H_{26}NORu]^+$ ([M − Cl]$^+$): m/z 482.1060. Found: m/z 482.1072.

Synthesis of the Half-Sandwich Ruthenium Complex ***4b***. **Method A** (mechanochemical synthesis method): [(4-Chlorophenyl)methyl]triphenylphosphonium (84.7 mg, 0.2 mmol) and potassium *tert*-butoxide (33.7 mg, 0.3 mmol) were manually ground in a mortar with a pestle for 1 min until a yellow solid was obtained. Then, **2** (42.7 mg, 0.1 mmol) was added to the solid mixture and grinding was continued for 1 h in the presence of 2 droplets of CH_2Cl_2. The resulting products was poured into a CH_2Cl_2 solution, the unsolved precipitate was removed by filtration, and the solvent was removed under vacuum. The mixture was passed through a short pad of silica gel with hexane and isopropyl alcohol to give the ruthenium complex **4b** (33.7 mg, 61%). **Method A** (mechanochemical synthesis method): $[Ru(p\text{-cymene})(\mu\text{-Cl})Cl]_2$ (61.2 mg, 0.10 mmol), **3b** (0.2 mmol), and K_2CO_3 (27.6 mg, 0.2 mmol) were manually ground in a mortar with a pestle for 20 min in the presence of 5 droplets of CH_2Cl_2. The resulting products were poured into a CH_2Cl_2 solution, the unsolved precipitate was removed by filtration, and the solvent was removed in vacuo. The mixture was passed through a short pad of silica gel with hexane and isopropyl alcohol to give the ruthenium complex **4b** (102.9 mg, 93%). **Method B** (solution method): A solution of $[Ru(p\text{-cymene})(\mu\text{-Cl})Cl]_2$ (61.2 mg, 0.10 mmol), **3b** (0.22 mmol), and K_2CO_3 (35.4 mg, 0.22 mmol) in methanol (5 mL) was purged with nitrogen and then stirred at 70 °C for 2 h. After it was cooled to room temperature, the solvent was removed under vacuum (rotary evaporator). The mixture was passed through a short pad of silica gel with ethyl acetate and petroleum ether (2:1) to give the dark-red half-sandwich ruthenium complex **4b** (64.0 mg, 58%). ^{1}H NMR (500 MHz, $CDCl_3$): δ 8.10 (d, J = 16 Hz, 1 H), 8.03 (d, J = 12 Hz, 1 H), 7.68 (d, J = 8 Hz, 1 H), 7.62 (d, J = 8 Hz, 2 H), 7.48 (d, J = 8 Hz, 2 H), 7.33 (d, J = 8 Hz, 1 H), 7.29 (d, J = 8 Hz, 1 H), 7.02 (d, J = 8 Hz, 1 H), 6.79 (d, J = 8 Hz, 1 H), 5.62 (d, J = 4 Hz, 1 H), 5.52 (d, J = 4 Hz, 1 H), 5.36 (d, J = 8 Hz, 1 H), 5.09 (d, J = 8 Hz, 1 H), 2.56 (m, 1 H), 2.32 (s, 3 H), 1.03 (d, J = 8 Hz, 3 H), 0.94 (d, J = 4 Hz, 3 H). ^{13}C NMR (125 MHz, $CDCl_3$): δ 168.9, 155.9, 144.8, 137.9, 135.4, 134.8, 132.9, 131.9, 130.2, 129.9, 129.0, 128.9, 120.2, 116.2, 111.0, 101.9, 100.5, 85.9, 81.4, 81.2, 80.8, 31.2, 22.6, 22.4, 19.3. IR (KBr cm^{-1}): 3435 (m), 3045 (w), 2961 (m), 2921 (m), 2851 (w), 1737 (vw), 1625 (w), 1593 (w), 1550 (s), 1490 (m), 1439 (s), 1403 (m), 1372 (s), 1330 (m), 1296 (m), 1260 (m), 1105 (s), 1035 (m), 1012 (m), 975 (w), 869 (w), 831 (s), 808 (m), 736 (w), 540 (w). Anal. Calcd for $C_{27}H_{25}NORuCl_2$: C, 58.81; H, 4.57; N, 2.54. Found: C, 58.84; H, 4.52; N, 2.59. ESI-MS. Calcd for $[C_{27}H_{25}ClNORu]^+$ ([M − Cl]$^+$): m/z 516.0667. Found: m/z 516.0703.

General Procedure for Transfer Hydrogenation of Ketone Compounds with a Half-Sandwich Ruthenium Complex. A mixture of ketone compounds (0.1 mmol), MeONa (0.4 mmol, 4 equiv), and a half-sandwich ruthenium complex (0.25 mol %) in 2-propanol (1.0 mL) was heated to 80 °C for 12 h. After the reaction had completed (monitored by thin-layer chromatography), the reaction mixture was cooled to room temperature. Then, the solvent was removed under reduced pressure and extracted with ethyl acetate and water (3× 5 mL). The organic layers were analyzed by GC−MS using *n*-dodecane as an internal standard.

X-ray Structure Determination. The diffraction data of **2**, **4a**, and **4b** were collected on a Bruker AXS SMART APEX diffractometer, equipped with a CCD area detector using Mo Kα radiation (λ = 0.71073 Å). All of the data were collected at 298 K, and the structures were solved by direct methods and subsequently refined on F^2 by using full-matrix least-squares techniques (*SHELXL*).[59] *SADABS*[60] absorption corrections were applied to the data, all non-hydrogen atoms were refined anisotropically, and hydrogen atoms were located at calculated positions. All calculations were performed using the Bruker *SMART* program.

■ ASSOCIATED CONTENT

Supporting Information

The Supporting Information is available free of charge at https://pubs.acs.org/doi/10.1021/acs.inorgchem.1c00059.

NMR data and IR spectra of the half-sandwich ruthenium complexes and computational details (PDF)

Accession Codes

CCDC 2036546−2036548 contain the supplementary crystallographic data for this paper. These data can be obtained free of charge via www.ccdc.cam.ac.uk/data_request/cif, or by emailing data_request@ccdc.cam.ac.uk, or by contacting The Cambridge Crystallographic Data Centre, 12 Union Road, Cambridge CB2 1EZ, UK; fax: +44 1223 336033.

■ AUTHOR INFORMATION

Corresponding Authors

Wei-Guo Jia − *The Key Laboratory of Functional Molecular Solids, Ministry of Education, Anhui Laboratory of Molecular-Based Materials (State Key Laboratory Cultivation Base), College of Chemistry and Materials Science, Anhui Normal University, Wuhu 241002, China; State Key Laboratory of Structural Chemistry, Fujian Institute of Research on the Structure of Matter, Chinese Academy of Science, Fuzhou 350002, China;* orcid.org/0000-0001-7976-7543; Email: wgjiasy@mail.ahnu.edu.cn

Richmond Lee − *School of Chemistry and Molecular Bioscience and Molecular Horizons, University of Wollongong, Wollongong, New South Wales 2522, Australia;* orcid.org/0000-0003-1264-4914; Email: richmond_lee@uow.edu.au

Authors

Xue-Ting Zhi − *The Key Laboratory of Functional Molecular Solids, Ministry of Education, Anhui Laboratory of Molecular-Based Materials (State Key Laboratory Cultivation Base), College of Chemistry and Materials Science, Anhui Normal University, Wuhu 241002, China*

Xiao-Dong Li − *The Key Laboratory of Functional Molecular Solids, Ministry of Education, Anhui Laboratory of Molecular-Based Materials (State Key Laboratory Cultivation Base), College of Chemistry and Materials Science, Anhui Normal University, Wuhu 241002, China*

Jun-Peng Zhou − *The Key Laboratory of Functional Molecular Solids, Ministry of Education, Anhui Laboratory of Molecular-Based Materials (State Key Laboratory Cultivation Base), College of Chemistry and Materials Science, Anhui Normal University, Wuhu 241002, China*

Rui Zhong − *The Key Laboratory of Functional Molecular Solids, Ministry of Education, Anhui Laboratory of Molecular-Based Materials (State Key Laboratory Cultivation Base), College of Chemistry and Materials Science, Anhui Normal University, Wuhu 241002, China*

Haibo Yu − *School of Chemistry and Molecular Bioscience and Molecular Horizons, University of Wollongong, Wollongong, New South Wales 2522, Australia;* orcid.org/0000-0002-1099-2803

https://doi.org/10.1021/acs.inorgchem.1c00059
Inorg. Chem. 2021, 60, 4313−4321

Complete contact information is available at:
https://pubs.acs.org/10.1021/acs.inorgchem.1c00059

Notes

The authors declare no competing financial interest.

■ ACKNOWLEDGMENTS

We acknowledge financial support from the National Natural Science Foundation of China (Grant 21102004), Australian Research Council (DECRA Award DE210100053), University of Wollongong (VC Fellowship), and National Computing Infrastructure (Australia) for computing resources. We also thank Dr. Davin Tan for helpful discussions and suggestions.

■ REFERENCES

(1) James, S. L.; Adams, C. J.; Bolm, C.; Braga, D.; Collier, P.; Friščić, T.; Grepioni, F.; Harris, K. D. M.; Hyett, G.; Jones, W.; Krebs, A.; Mack, J.; Maini, L.; Orpen, A. G.; Parkin, I. P.; Shearouse, W. C.; Steed, J. W.; Waddell, D. C. Mechanochemistry: opportunities for new and cleaner synthesis. *Chem. Soc. Rev.* **2012**, *41* (1), 413−447.

(2) Beillard, A.; Bantreil, X.; Métro, T.-X.; Martinez, J.; Lamaty, F. Alternative Technologies That Facilitate Access to Discrete Metal Complexes. *Chem. Rev.* **2019**, *119* (12), 7529−7609.

(3) Porcheddu, A.; Colacino, E.; De Luca, L.; Delogu, F. Metal-Mediated and Metal-Catalyzed Reactions Under Mechanochemical Conditions. *ACS Catal.* **2020**, *10*, 8344−8394.

(4) Friščić, T.; Mottillo, C.; Titi, H. M. Mechanochemistry for Synthesis. *Angew. Chem., Int. Ed.* **2020**, *59*, 1018−1029.

(5) Do, J.-L.; Friščić, T. Mechanochemistry: A Force of Synthesis. *ACS Cent. Sci.* **2017**, *3*, 13−19.

(6) Pétry, N.; Vanderbeeken, T.; Malher, A.; Bringer, Y.; Retailleau, P.; Bantreil, X.; Lamaty, F. Mechanosynthesis of sydnone-containing coordination complexes. *Chem. Commun.* **2019**, *55* (64), 9495−9498.

(7) Garra, P.; Dumur, F.; Mokbel, H.; Monnier, V.; Morlet-Savary, F.; Dietlin, C.; Gigmes, D.; Fouassier, J.-P.; Lalevée, J. New Synthetic Route to an Highly Efficient Photoredox Catalyst by Mechanosynthesis. *ACS Omega* **2018**, *3* (9), 10938−10944.

(8) Raje, S.; Angamuthu, R. Solvent-free synthesis and reactivity of nickel(II) borohydride and nickel(II) hydride. *Green Chem.* **2019**, *21* (10), 2752−2758.

(9) Seki, T.; Jin, M.; Ito, H. Introduction of a Biphenyl Moiety for a Solvent-Responsive Aryl Gold(I) Isocyanide Complex with Mechanical Reactivation. *Inorg. Chem.* **2016**, *55*, 12309−12320.

(10) Seki, T.; Tokodai, N.; Omagari, S.; Nakanishi, T.; Hasegawa, Y.; Iwasa, T.; Taketsugu, T.; Ito, H. Luminescent Mechanochromic 9-Anthryl Gold(I) Isocyanide Complex with an Emission Maximum at 900 nm after Mechanical Stimulation. *J. Am. Chem. Soc.* **2017**, *139*, 6514−6517.

(11) Ayoub, G.; Karadeniz, B.; Howarth, A. J.; Farha, O. K.; Đilović, I.; Germann, L. S.; Dinnebier, R. E.; Užarević, K.; Friščić, T. Rational Synthesis of Mixed-Metal Microporous Metal-Organic Frameworks with Controlled Composition Using Mechanochemistry. *Chem. Mater.* **2019**, *31* (15), 5494−5501.

(12) Prochowicz, D.; Sokołowski, K.; Justyniak, I.; Kornowicz, A.; Fairen-Jimenez, D.; Friščić, T.; Lewiński, J. A mechanochemical strategy for IRMOF assembly based on pre-designed oxo-zinc precursors. *Chem. Commun.* **2015**, *51* (19), 4032−4035.

(13) Crawford, D.; Casaban, J.; Haydon, R.; Giri, N.; McNally, T.; James, S. L. Synthesis by extrusion: continuous, large-scale preparation of MOFs using little or no solvent. *Chem. Sci.* **2015**, *6* (3), 1645−1649.

(14) Biswal, B. P.; Chandra, S.; Kandambeth, S.; Lukose, B.; Heine, T.; Banerjee, R. Mechanochemical Synthesis of Chemically Stable Isoreticular Covalent Organic Frameworks. *J. Am. Chem. Soc.* **2013**, *135* (14), 5328−5331.

(15) Bosch, E.; Kruse, S. J.; Krueger, H. R.; Groeneman, R. H. Role of $\pi-\pi$ Stacking and Halogen Bonding by 1,4-Diiodoperchlorobenzene To Organize the Solid State To Achieve a [2 + 2] Cycloaddition Reaction. *Cryst. Growth Des.* **2019**, *19* (6), 3092−3096.

(16) Sokolov, A. N.; Bučar, D.-K.; Baltrusaitis, J.; Gu, S. X.; MacGillivray, L. R. Supramolecular Catalysis in the Organic Solid State through Dry Grinding. *Angew. Chem., Int. Ed.* **2010**, *49* (25), 4273−4277.

(17) Yuan, S.; Liu, S.-S.; Sun, D. Two isomeric $[Cu_4I_4]$ luminophores: solvothermal/mechanochemical syntheses, structures and thermochromic luminescence properties. *CrystEngComm* **2014**, *16* (10), 1927−1933.

(18) Kobayashi, A.; Yoshida, Y.; Yoshida, M.; Kato, M. Mechanochromic Switching between Delayed Fluorescence and Phosphorescence of Luminescent Coordination Polymers Composed of Dinuclear Copper(I) Iodide Rhombic Cores. *Chem. - Eur. J.* **2018**, *24* (55), 14750−14759.

(19) Grifasi, F.; Chierotti, M. R.; Garino, C.; Gobetto, R.; Priola, E.; Diana, E.; Turci, F. Solvent-Free Synthesis of Luminescent Copper(I) Coordination Polymers with Thiourea Derivatives. *Cryst. Growth Des.* **2015**, *15* (6), 2929−2939.

(20) Beillard, A.; Métro, T.-X.; Bantreil, X.; Martinez, J.; Lamaty, F. Cu(0), O_2 and mechanical forces: a saving combination for efficient production of Cu-NHC complexes. *Chem. Sci.* **2017**, *8* (2), 1086−1089.

(21) Mukherjee, N.; Marczyk, A.; Szczepaniak, G.; Sytniczuk, A.; Kajetanowicz, A.; Grela, K. A Gentler Touch: Synthesis of Modern Ruthenium Olefin Metathesis Catalysts Sustained by Mechanical Force. *ChemCatChem* **2019**, *11* (21), 5362−5369.

(22) Kubota, K.; Takahashi, R.; Ito, H. Mechanochemistry allows carrying out sensitive organometallic reactions in air: glove-box-and-Schlenk-line-free synthesis of oxidative addition complexes from aryl halides and palladium(0). *Chem. Sci.* **2019**, *10* (22), 5837−5842.

(23) Hernández, J. G.; Butler, I. S.; Friščić, T. Multi-step and multi-component organometallic synthesis in one pot using orthogonal mechanochemical reactions. *Chem. Sci.* **2014**, *5* (9), 3576−3582.

(24) Rightmire, N. R.; Hanusa, T. P. Advances in organometallic synthesis with mechanochemical methods. *Dalton Trans.* **2016**, *45* (6), 2352−2362.

(25) Boyde, N. C.; Steelman, G. W.; Hanusa, T. P. Multicomponent Mechanochemical Synthesis of Cyclopentadienyl Titanium tert-Butoxy Halides, $CpxTiXy(OtBu)_{4-(x+y)}$ (x, y = 1, 2; X = Cl, Br). *ACS Omega* **2018**, *3*, 8149−8159.

(26) Koby, R. F.; Hanusa, T. P.; Schley, N. D. Mechanochemically Driven Transformations in Organotin Chemistry: Stereochemical Rearrangement, Redox Behavior, and Dispersion-Stabilized Complexes. *J. Am. Chem. Soc.* **2018**, *140*, 15934−15942.

(27) Liang, P.; Kobayashi, A.; Hasegawa, T.; Yoshida, M.; Kato, M. Thermal and Mechanochemical Syntheses of Luminescent Mononuclear Copper(I) Complexes. *Eur. J. Inorg. Chem.* **2017**, *2017* (44), 5134−5142.

(28) Seo, T.; Kubota, K.; Ito, H. Selective Mechanochemical Monoarylation of Unbiased Dibromoarenes by in Situ Crystallization. *J. Am. Chem. Soc.* **2020**, *142*, 9884−9889.

(29) Ingner, F. J. L.; Giustra, Z. X.; Novosedlik, S.; Orthaber, A.; Gates, P. J.; Dyrager, C.; Pilarski, L. T. Mechanochemical synthesis of (hetero)aryl Au(I) complexes. *Green Chem.* **2020**, *22*, 5648−5655.

(30) Quintin, F.; Pinaud, J.; Lamaty, F.; Bantreil, X. Mechanosynthesis of Noels-type NHC-Ruthenium Complexes and Applications in Ring-Opening Metathesis Polymerization. *Organometallics* **2020**, *39*, 636−639.

(31) Quintin, F.; Pinaud, J.; Lamaty, F.; Bantreil, X. Mechanosynthesis of Noels-type NHC−Ruthenium Complexes and Applications in Ring-Opening Metathesis Polymerization. *Organometallics* **2020**, *39* (5), 636−639.

(32) Shaw, T. E.; Mathivathanan, L.; Jurca, T. One-Pot, One-Step Precatalysts through Mechanochemistry. *Organometallics* **2019**, *38* (21), 4066−4070.

(33) Gao, W.-X.; Feng, H.-J.; Guo, B.-B.; Lu, Y.; Jin, G.-X. Coordination-Directed Construction of Molecular Links. *Chem. Rev.* **2020**, *120*, 6288−6325.

(34) Lu, Y.; Zhang, H.-N.; Jin, G.-X. Molecular Borromean Rings Based on Half-Sandwich Organometallic Rectangles. *Acc. Chem. Res.* **2018**, *51*, 2148−2158.
(35) Han, Y.-F.; Jia, W.-G.; Yu, W.-B.; Jin, G.-X. Stepwise formation of organometallic macrocycles, prisms and boxes from Ir, Rh and Ru-based half-sandwich units. *Chem. Soc. Rev.* **2009**, *38*, 3419−3434.
(36) Jia, W.-G.; Zhang, T.; Xie, D.; Xu, Q.-T.; Ling, S.; Zhang, Q. Half-sandwich cycloruthenated complexes from aryloxazolines: synthesis, structures, and catalytic activities. *Dalton Trans.* **2016**, *45* (36), 14230−14237.
(37) Jia, W.-G.; Ling, S.; Zhang, H.-N.; Sheng, E.-H.; Lee, R. Half-Sandwich Ruthenium Phenolate-Oxazoline Complexes: Experimental and Theoretical Studies in Catalytic Transfer Hydrogenation of Nitroarene. *Organometallics* **2018**, *37* (1), 40−47.
(38) Lin, N.; Ou, H.-D.; Xu, Q.; Jin, Y.; Deng, W.; Yao, Z.-J. An Efficient Probe of Cyclometallated Phosphorescent Iridium Complex for Selective Detection of Cyanide. *ACS Omega* **2020**, *5* (9), 4636−4645.
(39) Lo, K. K.-W.; Lau, J. S.-Y. Cyclometalated Iridium(III) Diimine Bis(biotin) Complexes as the First Luminescent Biotin-Based Cross-Linkers for Avidin. *Inorg. Chem.* **2007**, *46* (3), 700−709.
(40) Jiao, L.; Yu, C.; Li, J.; Wang, Z.; Wu, M.; Hao, E. β-Formyl-BODIPYs from the Vilsmeier-Haack Reaction. *J. Org. Chem.* **2009**, *74* (19), 7525−7528.
(41) Wang, J.; Wu, Y.; Sheng, W.; Yu, C.; Wei, Y.; Hao, E.; Jiao, L. Synthesis, Structure, and Properties of β-Vinyl Ketone/Ester Functionalized AzaBODIPYs from FormylazaBODIPYs. *ACS Omega* **2017**, *2* (6), 2568−2576.
(42) Balema, V. P.; Wiench, J. W.; Pruski, M.; Pecharsky, V. K. Mechanically Induced Solid-State Generation of Phosphorus Ylides and the Solvent-Free Wittig Reaction. *J. Am. Chem. Soc.* **2002**, *124* (22), 6244−6245.
(43) Jia, W.-G.; Cheng, M.-X.; Xu, Q.-T.; Gao, L.-L.; Yuan, G. Synthesis of six 8-quinolinate-based ruthenium complexes with high catalytic activity for nitroarene reduction. *Polyhedron* **2018**, *153*, 69−75.
(44) Gemel, C.; John, R.; Slugovc, C.; Mereiter, K.; Schmid, R.; Kirchner, K. Synthesis and characterization of ruthenium quinolin-8-olate complexes. Unexpected formation of a κ^1-hydrotris(pyrazolyl)-borate complex. *J. Chem. Soc., Dalton Trans.* **2000**, *29* (15), 2607−2612.
(45) Schuecker, R.; John, R. O.; Jakupec, M. A.; Arion, V. B.; Keppler, B. K. Water-Soluble Mixed-Ligand Ruthenium(II) and Osmium(II) Arene Complexes with High Antiproliferative Activity. *Organometallics* **2008**, *27* (24), 6587−6595.
(46) Gobec, M.; Kljun, J.; Sosic, I.; Mlinaric-Rascan, I.; Ursic, M.; Gobec, S.; Turel, I. Structural characterization and biological evaluation of a clioquinol-ruthenium complex with copper-independent antileukaemic activity. *Dalton Trans.* **2014**, *43* (24), 9045−9051.
(47) Kubanik, M.; Holtkamp, H.; Söhnel, T.; Jamieson, S. M. F.; Hartinger, C. G. Impact of the Halogen Substitution Pattern on the Biological Activity of Organoruthenium 8-Hydroxyquinoline Anticancer Agents. *Organometallics* **2015**, *34* (23), 5658−5668.
(48) Han, Y.-F.; Li, H.; Fei, Y.; Lin, Y.-J.; Zhang, W.-Z.; Jin, G.-X. Synthesis and structural characterization of binuclear half-sandwich iridium, rhodium and ruthenium complexes containing 4,4′-dipyridyldisulfide (4DPDS) ligands. *Dalton Trans.* **2010**, *39* (30), 7119−7124.
(49) Zhang, W.-Z.; Han, Y.-F.; Lin, Y.-J.; Jin, G.-X. Synthesis and characterization of molecular rectangles of half-sandwich p-cymene ruthenium complexes bearing oxamidato ligands. *Dalton Trans.* **2009**, *39*, 8426−8431.
(50) Jia, W.-G.; Zhang, H.; Zhang, T.; Xie, D.; Ling, S.; Sheng, E.-H. Half-Sandwich Ruthenium Complexes with Schiff-Base Ligands: Syntheses, Characterization, and Catalytic Activities for the Reduction of Nitroarenes. *Organometallics* **2016**, *35* (4), 503−512.
(51) Yun, X.-J.; Zhu, J.-W.; Jin, Y.; Deng, W.; Yao, Z.-J. Half-Sandwich Ruthenium Complexes for One-Pot Synthesis of Quinolines and Tetrahydroquinolines: Diverse Catalytic Activity in the Coupled Cyclization and Hydrogenation Process. *Inorg. Chem.* **2020**, *59*, 7841−7851.
(52) Hu, P.; Wang, F.; Jin, G.-X. Syntheses, Characterization, and Ethylene Polymerization of Half-Sandwich Zirconium Complexes with Tridentate Imino-Quinolinol Ligands. *Organometallics* **2011**, *30* (5), 1008−1012.
(53) Yuan, G.; Huo, Y.; Nie, X.; Jiang, H.; Liu, B.; Fang, X.; Zhao, F. Controllable supramolecular structures and luminescent properties of unique trimeric Zn(II) 8-hydroxyquinolinates tuned by functional substituents. *Dalton Trans.* **2013**, *42* (8), 2921−2929.
(54) Kharchenko, O.; Smokal, V.; Krupka, O.; Kolendo, A. Reactivity and polymerization ability of styrylquinoline containing methacrylic monomers. *Chem. Chem. Technol.* **2018**, *12* (1), 47−52.
(55) Yuan, G.; Zhang, Q.; Wang, Z.; Song, K.; Yuan, X.; Wang, Y.; Zhang, L. Assembly of four 8-quinolinate-based multinuclear complexes: the effect of substituents on core structures and photoluminescence properties. *Inorg. Chem. Front.* **2017**, *4* (5), 764−772.
(56) Musiol, R.; Jampilek, J.; Podeszwa, B.; Finster, J.; Tabak, D.; Dohnal, J.; Polanski, J. RP-HPLC determination of lipophilicity in series of quinoline derivatives. *Cent. Eur. J. Chem.* **2009**, *7* (3), 586−597.
(57) Knez, D.; Colettis, N.; Iacovino, L. G.; Sova, M.; Pišlar, A.; Konc, J.; Lešnik, S.; Higgs, J.; Kamecki, F.; Mangialavori, I.; Dolšak, A.; Žakelj, S.; Trontelj, J.; Kos, J.; Binda, C.; Marder, M.; Gobec, S. Stereoselective Activity of 1-Propargyl-4-styrylpiperidine-like Analogues That Can Discriminate between Monoamine Oxidase Isoforms A and B. *J. Med. Chem.* **2020**, *63* (3), 1361−1387.
(58) Chenna, B. C.; Li, L.; Mellott, D. M.; Zhai, X.; Siqueira-Neto, J. L.; Calvet Alvarez, C.; Bernatchez, J. A.; Desormeaux, E.; Alvarez Hernandez, E.; Gomez, J.; McKerrow, J. H.; Cruz-Reyes, J.; Meek, T. D. Peptidomimetic Vinyl Heterocyclic Inhibitors of Cruzain Effect Antitrypanosomal Activity. *J. Med. Chem.* **2020**, *63* (6), 3298−3316.
(59) Sheldrick, G. *SHELXL-97, a Program for Refining Crystal Structures*; University of Göttingen: Göttingen, Germany, 1997.
(60) Sheldrick, G. *SADABS v. 2.01, Bruker/Siemens Area Detector Absorption Correction Program*; Bruker AXS: Madison, WI, 1998.

https://doi.org/10.1021/acs.inorgchem.1c00059
Inorg. Chem. 2021, 60, 4313−4321